Fitting unanchored puzzle piece in the skeleton: spatial scapular position optimized for the steady support in quadrupedal tetrapods:

Supporting Information

Shin-ichi Fujiwara

The Nagoya University Museum, Furocho, Chikusa, Nagoya, 464-8601 Japan

---

Introduction

Materials and methods

Results

Rotation models

Appendix S1 Rotation model of *Felis* for SIMM 6.0.3.
Appendix S2 Rotation model of *Rattus* for SIMM 6.0.3.
Appendix S3 Rotation model of *Chamaeleo* for SIMM 6.0.3.
SIMM 6.0.3 (Musculographics Inc., Santa Rosa, USA) is required to be installed to open these files. Each data is composed of joint (JNT), muscle (MSL), and bone (ASC) files. They are compressed into RAR file format.

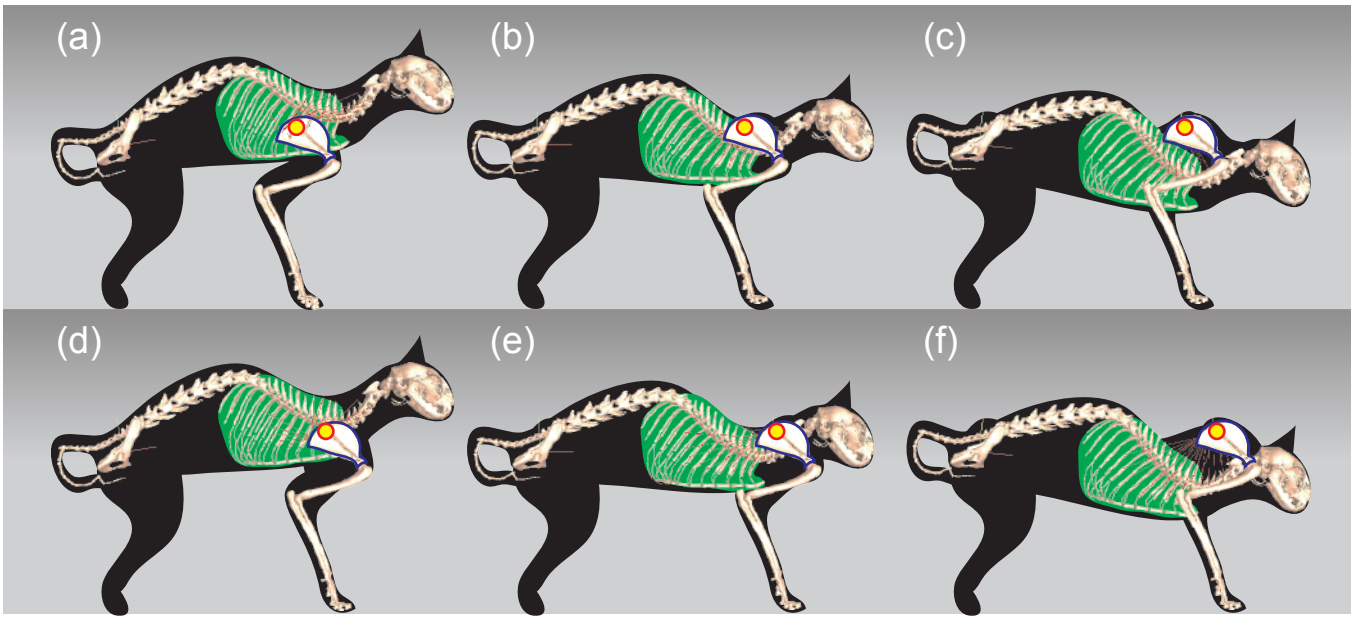

Fig. S1 Difference of the skeletal posture depending on the possible scapular positions to the rib cage in *Felis*. The scapulae are outlined in blue, and the rib cages are indicated in green. The top position of the scapulae were marked with the red circle filled with yellow. The skeletal postures excluding the scapular positions are same. The scapulae are respectively positioned at (a–c) posterior; (d–f) anterior; (a, d) ventral; (b, e) near the vertebral column; and (c, f) high above the vertebral column.

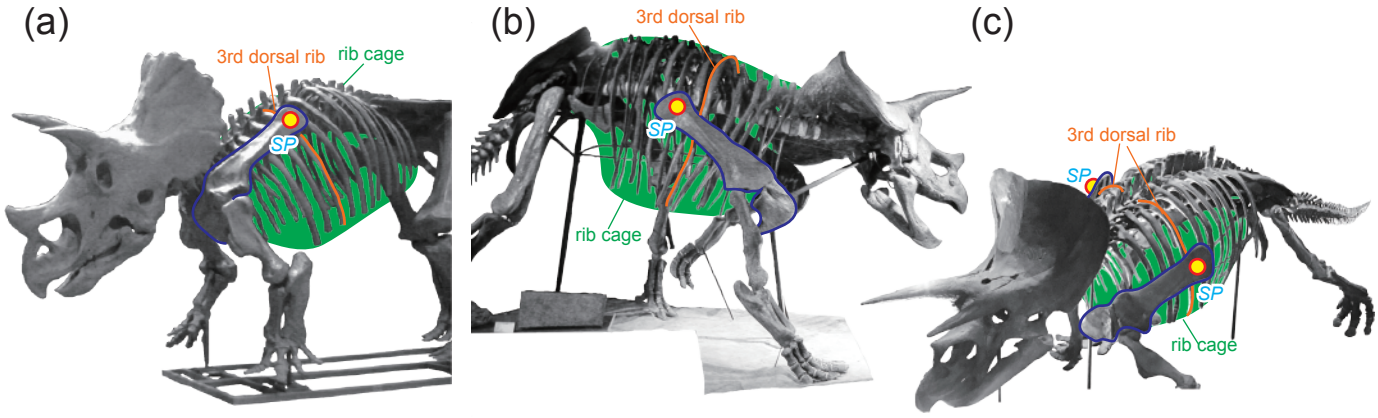

Fig. S2 Difference of the scapular positions (*SP*) among skeletal mounts of *Triceratop*s (Ceratopsia, Dinosauria). The top position of the scapulae were marked with the red circle filled with yellow. The positions of the rib cage indicated in green and the 3rd dorsal rib outlined in orange were shown for comparison. The skeletal mounts are (a) NSM PV unnumbered; (b) GMNH PV 124; and (c) KMNH, catalog no. 1985X22VP03. The scapulae are positioned cranio-dorso-medially in (a), caudo-ventro-laterally in (b), and cranio-ventro-laterally in (c). Institutional Abbreviations: GMNH, Gunma Museum of Natural History, Tomioka, Japan; KMNH, Kitakyushu Museum of Natural History, Kitakyushu, Japan; NSM, National Museum of Nature and Science, Tokyo, Japan.

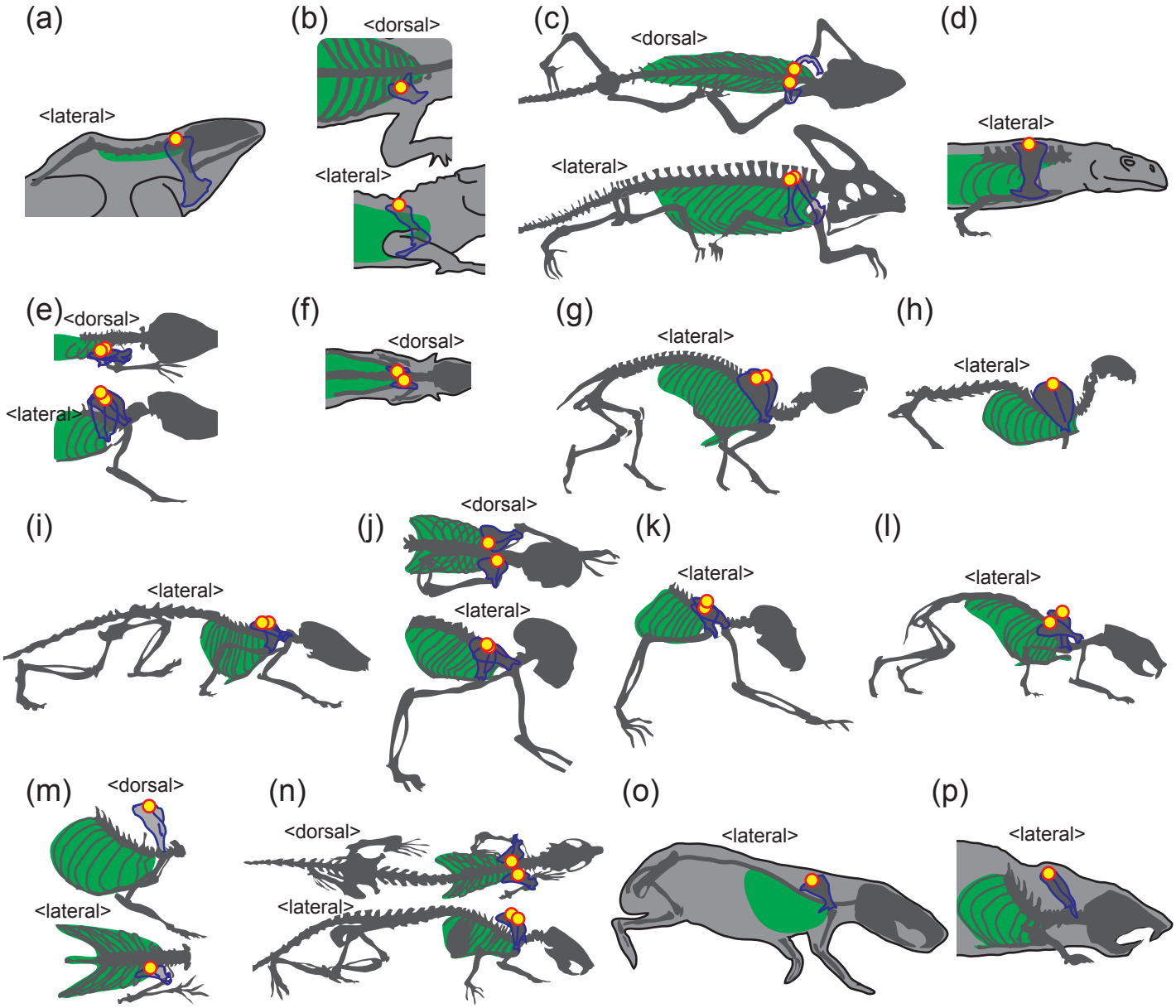

Fig. S3 Scapular positions shared by extant non-testudine quadrupedal tetrapods. The silhouettes of the animals in motions in the dorsal and the right lateral views were redrawn from the cineradiographic images. The scapulae/scapulocoracoids were outlined in blue, the trunks were coloured in green, and the top positions of the scapulae were marked with the red circles filled with yellow. (a) *Rana* (Jenkins & Shubin, 1998); (b) *Alligator* (Baier & Gatesy, 2013); (c) *Chamaeleo* (Fischer et al., 2010); (d) *Varanus* (Jenkins & Goslow, 1983); (e) *Didelphis* (Jenkins & Weijs, 1979); (f) *Monodelphis* (Pridmore, 1992); (g) *Procavia* (Fischer, 1994); (h) *Felis* (Macphersen & Ye, 1998); (i) *Tupaia* (Schilling & Fischer, 1999); (j) *Saimiri* (Scmidt, 2005); (k) *Eulemur* (Schmidt & Fischer, 2000); (l) *Ochotona* (Fischer & Lehman, 1998); (m) *Rattus* (Jenkins, 1974); (n) *Rattus* (Schmidt & Fischer, 2011); (o) *Cavia* (Rocha-Barbosa et al., 2005); (p) *Spalax* (Gambaryan et al., 2005). Taxonomic variations: (a) Anura; (b) Crocodylia; (c, d) Lepidosaurmorpha; (e, f) Didelphiomorphia; (g) Hyracoidea; (h) Carnivora; (i) Scandentia; (j, k) Primates; (l) Lagomorpha; (m–o) Rodentia. See References in the main text.

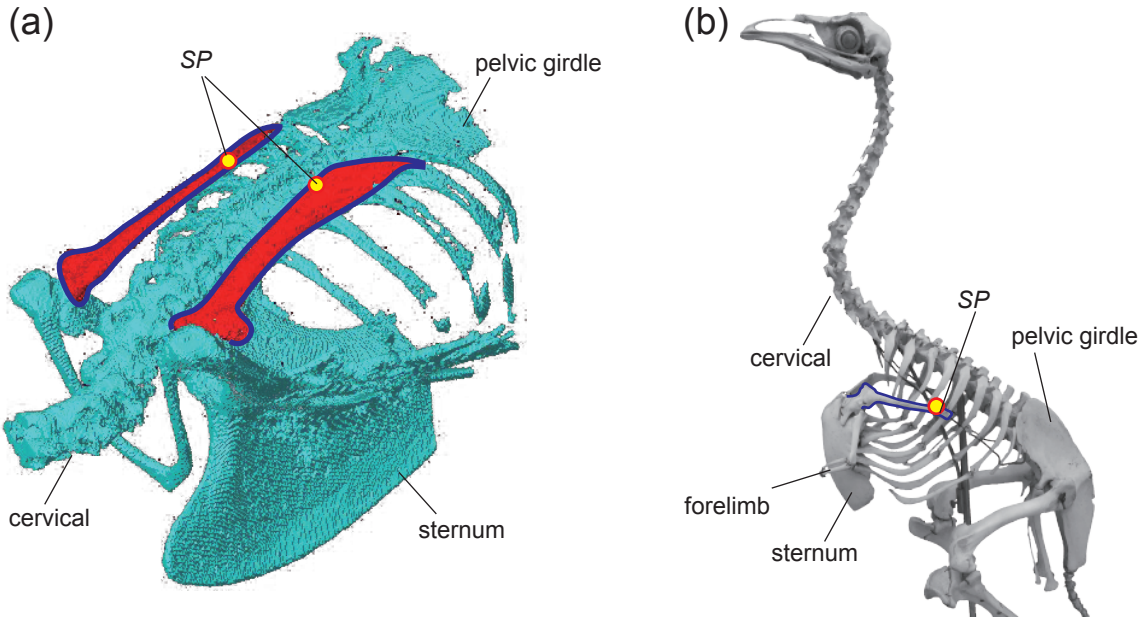

Fig. S4 Scapular positions (*SP*) in (a) flying (SIF unnumbered: *Columba livia*, Columbidae, Columbiformes, Aves) and (b) obligate bipedal (NUM unnumbered: *Casuarius* sp., Casuariidae, Casuariiformes, Aves) tetrapods. The scapulae are outlined in blue. Institutional abbreviations: NUM, The Nagoya University Museum, Nagoya University, Nagoya, Japan; SIF, personal collections of Shin-ichi Fujiwara, Nagoya University Museum, Nagoya, Japan.

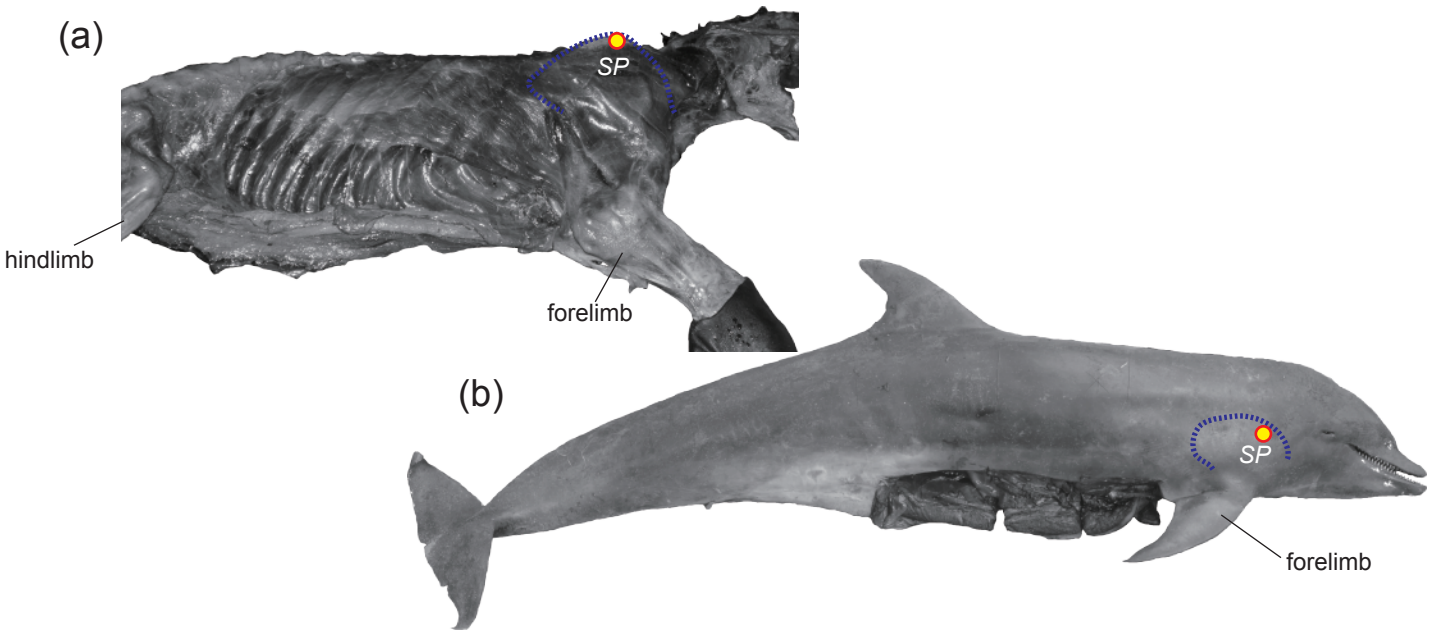

Fig. S5 Scapular positions (*SP*) in (a) semi-aquatic (UMUT unnumbered: *Callorhinus ursinus*, Otariidae, Carnivora, Mammalia) and (b) obligate aquatic (UMUT unnumbered: *Tursiops truncatus*, Delphinidae, Cetacea, Mammalia) tetrapods. The dorsal margins of the scapulae are indicated in blue dotted line. Institutional abbreviation: UMUT, The University Museum, The University of Tokyo, Tokyo, Japan.

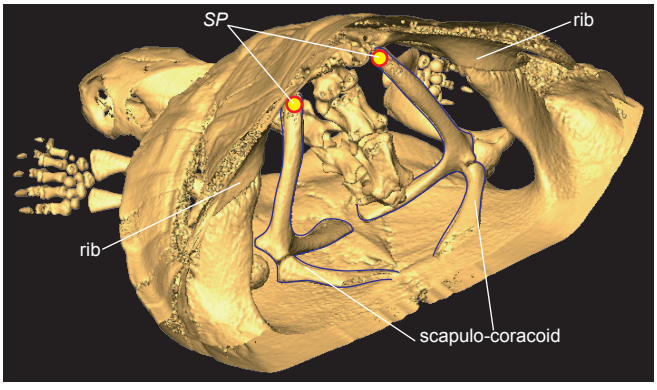

Fig. S6 Scapular positions of testudines. Anterior-half of *Mauremys japonica* (SIF 002) shown in caudo-lateral view. The top positions of the scapulae (*SP*) were marked with the red circles filled with yellow. Note that the scapulo-coracoid is positioned inside the rib cage (carapace). Institutional Abbreviation: SIF, personal collection of Shin-ichi Fujiwara, The Nagoya University Museum, Nagoya, Japan.

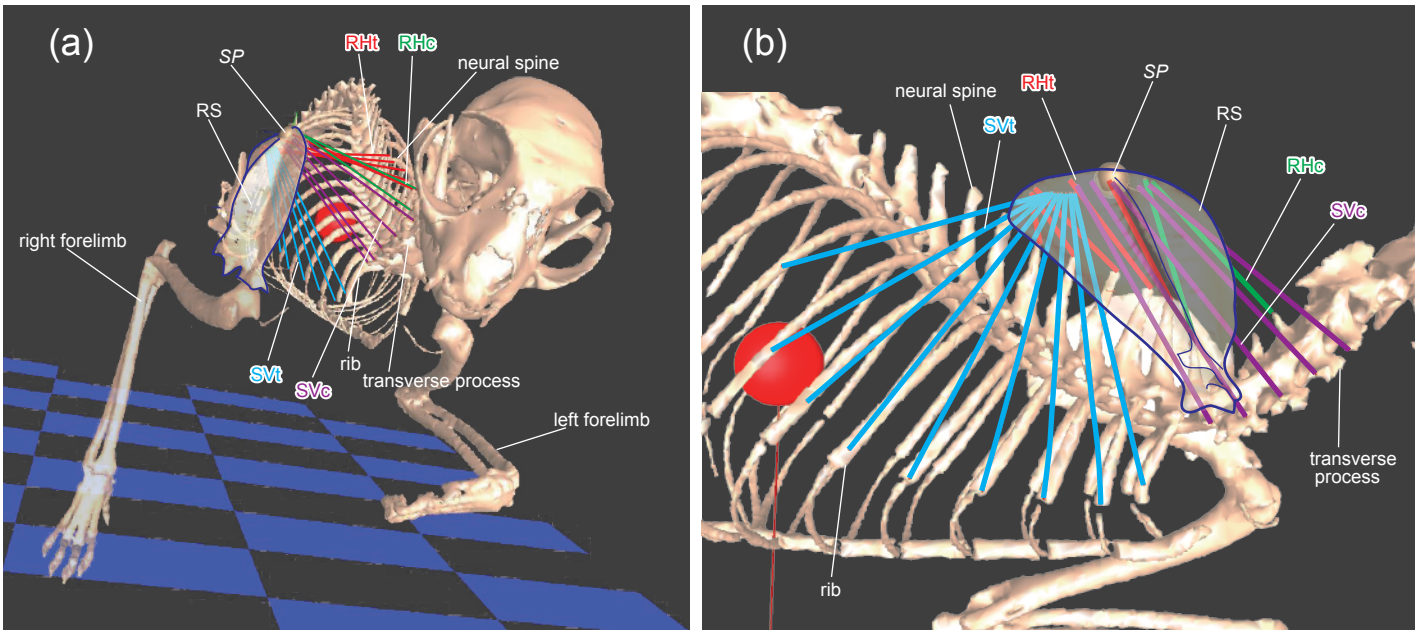

Fig. S7 Muscular connection between the scapula and rib cage in *Felis*. The skeleton is shown in (a) the cranial and (b) the right lateral views in perspective projection. The hindlimb skeletons are not visualized here. The scapular position (*SP*) was defined at the dorsal margin of the scapula. The fascicles of thoracic muscles (RHc, *m. rhomboideus cervicis*; RHt, *m. rhomboideus thoracis*; SVc, *m. serratus ventralis cervicis*; SVt, *m. serratus ventralis thoracis*) connecting the rib cage and right scapula (RS) are shown in lines of the different colour (RHc, green; RHt, red; SVc, purple; SVt, light blue). The RHc and RHt originates from the neural spines of the cervical and thoracic vertebrae, respectively; and the SVc and SVt originates from the transverse processes of the cervical vertebrae and lateral aspects of the anterior ribs, respectively. Note that all the thoracic muscle fascicles (RHc, RHt, SVc, and SVt) insert to the dorso-medial aspect (near *SP*) of the scapula.

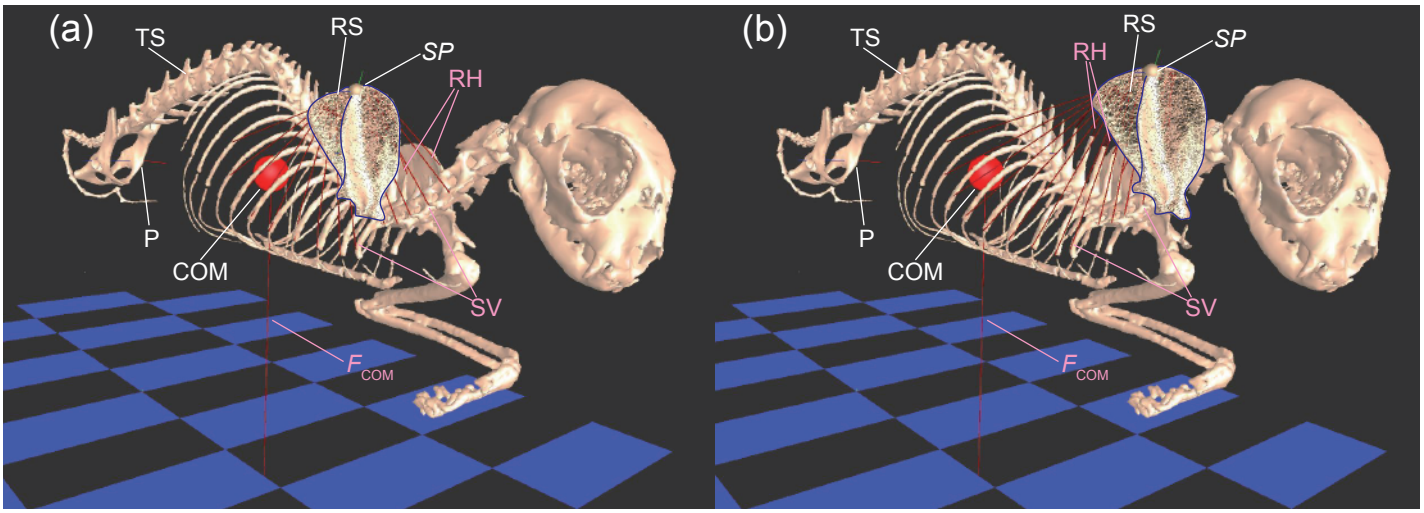

Fig. S8 The orientations of the muscle fascicles depending on the scapular positions. The right scapulae (RH) are in relatively (a) posterior and (b) anterior positions. The model assumes a stance on right forelimb and hindlimbs. The centre of mass (COM) of the uplifted portion of the body, which is composed of the skull, trunk, and the left forelimb, is subjected to gravitational force (F_{COM}). The scapular position (*SP*) was defined as the point on the top position of the scapula, the point where the *m. rhomboideus* (RH) and *m. serratus ventralis* (SV) insert. Note that the orientations of the paths of muscle fascicles (RH and SV) depend on the scapular position (*SP*). Abbreviations: P, a common pivot of the uplifted portion of the body and the thoracic skeleton (TS) about the acetabulum; RS, right scapula. The images were shown in the perspective projections. The three-dimensional musculoskeletal model was constructed using SIMM 6.0.3 (Musculographics Inc.).

Table S1 The specimens and CT scans used in this study. The scan resolution indicates the slice pitch and the pixel length of the CT scanned images.

taxa	specimen	body mass	CT scan	scan resolution	Institution
Felis catus	SIF 005	2.6 kg	TSX-021B/4B	1 mm	UMUT
Rattus norvegicus	SIF 012	74.5 g	Latheta LCT-100	0.25 mm	NMNS, Tsukuba
Chamaeleo melleri	KPM NFR476	335 g	TXS320-ACTIS	0.1 mm	NMNS, Tokyo

CT scan: Latheta LCT-100, Hitachi Aloca Medical, Ltd., Mitaka, Japan; TSX-021B/4B, Toshiba Medical Systems Co., Ltd., Otawara, Japan; TXS320-ACTIS, Tesco Co., Ltd., Tokyo, Japan.
Institution: KPM, Kanagawa Prefectural Museum, Odawara, Japan; NMNS, National Museum of Nature and Science, Tsukuba/Tokyo, Japan; SIF, personal collections of Shin-ichi Fujiwara, The Nagoya University Museum, Nagoya, Japan; UMUT, The University Museum, The University of Tokyo, Tokyo, Japan.

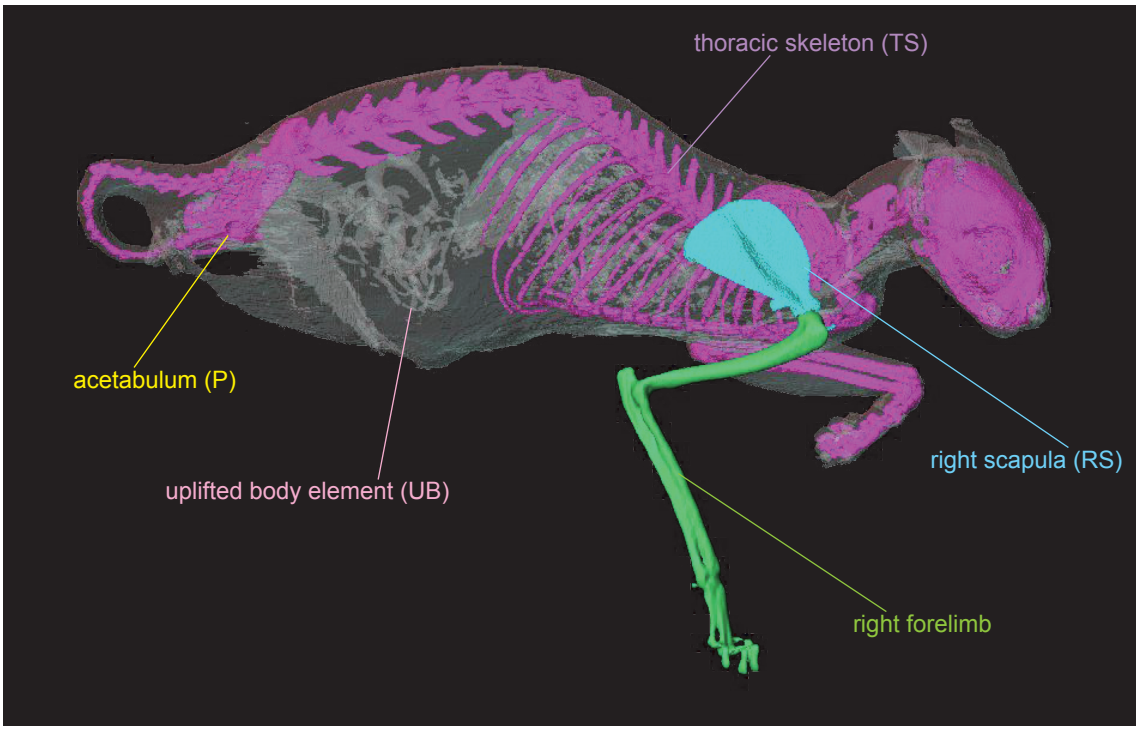

Fig. S9 Posture of the CT scanned specimen (*Felis*). The specimens were posed in posture during the stance on right forelimb and hindlimbs. The CT scanned data were used to reconstruct three-dimensional polygons of the body uplifted by the right forelimb and hindlimbs (UB), the thoracic skeleton (TS), and the right scapula (RS). This image was shown in the orthogonal projection. The segmentation was conducted using Avizo 8.1 (FEI Visualization Sciences Group).

Table S2 The forces applied to each muscle fascicle (F_{max}) and to the centre of mass (COM) of the uplifted body (F_{COM}) in the rotation model. The F_{max} was estimated by the physiological cross section area of the fascicle. Abbreviations for "muscle/force" are as follows: F_{COM}, product of the mass of uplifted body elements and gravity acceleration; LS, *m. levator scapulae*; RHc, *m. rhomboideus cervicis*; RHt, *m. rhomboideus thoracis*; SVc, *m. serratus ventralis cervicis*; SVt, *m. serratus ventralis thoracis*; TR, *m. trapezius*.

taxa	specimen	muscle/force	fascicle origin	force (N)
Felis catus	SIF 005	SVc	3rd cervical, transverse process	2.559
			4th cervical, transverse process	2.733
			5th cervical, transverse process	3.886
			6th cervical, transverse process	3.817
			7th cervical, transverse process	3.462
		SVt	1st thoracic rib, distal end	4.320
			2nd thoracic rib, distal end	2.029
			3rd thoracic rib, distal end	1.060
			4th thoracic rib, distal end	1.778
			5th thoracic rib, distal end	1.807
			6th thoracic rib, distal end	4.086
			7th thoracic rib, distal one-eighth	3.534
			8th thoracic rib, distal one-fifth	2.734
			9th thoracic rib, distal two-fifth	1.406
		RHc	3rd–7thcervical, neural spine, distal end	6.963
		RHt	1st thoracic, neural spine, distal end	3.887
			2nd thoracic, neural spine, distal end	3.994
			3rd thoracic, neural spine, distal end	2.415
			4th thoracic, neural spine, distal end	1.664
			5th thoracic, neural spine, distal end	1.272
		$1 \times F_{COM}$	COM	25.497
		$2 \times F_{COM}$	COM	50.995
		$3 \times F_{COM}$	COM	76.492
Rattus norvegicus	SIF 012	LS	occipital	0.173
		SVc	3rd cervical, transverse process	0.025
			4th cervical, transverse process	0.025
			5th cervical, transverse process	0.025
			6th cervical, transverse process	0.025
			7th cervical, transverse process	0.025
		SVt	1st thoracic rib, distal one-third	0.112
			1st thoracic rib, distal end	0.119
			2nd thoracic rib, distal end	0.093
			3rd thoracic rib, distal end	0.100
			4th thoracic rib, distal end	0.092
			5th thoracic rib, distal end	0.112
			6th thoracic rib, distal end	0.095
		RHt	2nd thoracic, neural spine, distal end	0.319
		$1 \times F_{COM}$	COM	0.731
		$2 \times F_{COM}$	COM	1.461
		$3 \times F_{COM}$	COM	2.192
Chamaeleo melleri	KPM NFR476	SVc	2nd cervical, rib distal end	4.168
			4th cervical rib, distal half	0.787
			4th cervical rib, distal three-eighth	0.668
			4th cervical rib, distal end	1.060
			5th cervical rib, distal end	1.046
		SVt	1st thoracic rib, distal one-fifth	0.954
			2nd thoracic rib, distal one-third	0.840
		TR	2nd thoracic, neural spine, distal four-fifth	0.847
		$1 \times F_{COM}$	COM	3.285
		$2 \times F_{COM}$	COM	6.570
		$3 \times F_{COM}$	COM	9.856
		$4 \times F_{COM}$	COM	13.141

Institutional abbreviations: KPM, Kanagawa Prefectural Museum of Natural History, Odawara, Japan; SIF, personal collections of S.-i. Fujiwara, Nagoya University Museum, Nagoya, Japan.

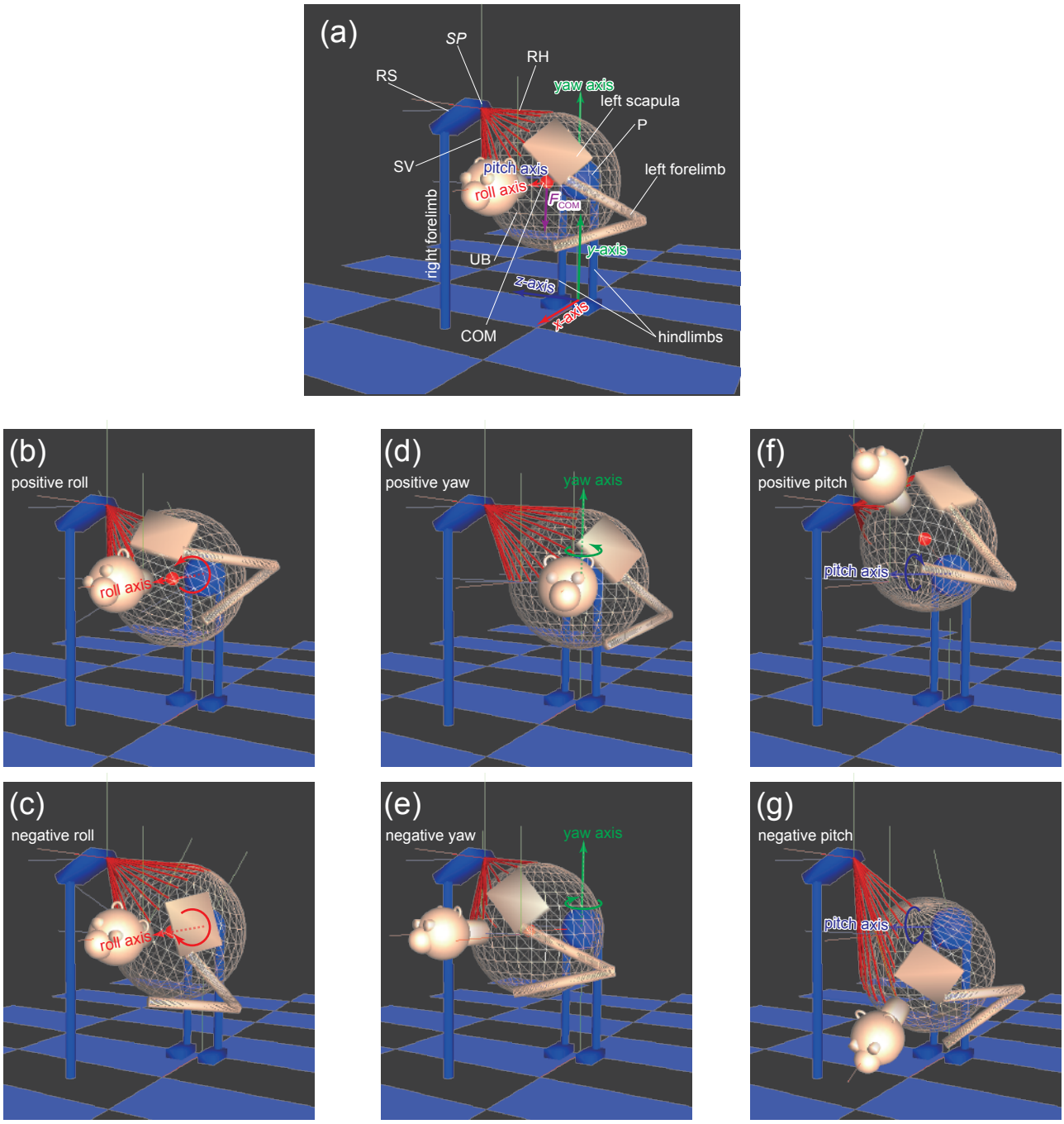

Fig. S10 Definitions of the rotational (roll, yaw, and pitch) axes of the uplifted body element (UB) in this study. The musculoskeletal model was constructed in the *x*, *y*, *z* coordinate space. The *x*-, *y*-, and *z*-axes, respectively correspond to longitudinal, vertical, and transverse orientations. The model assumes the support on the right forelimb and hindlimbs, and UB, which is composed of the head, trunk, and the left forelimb, is allowed to rotate three-dimensionally about the pivot on the acetabulum (P). Roll axis was defined as the line through the point P and centre of mass (COM) of the UB. Yaw axis was defined as the line perpendicular to the roll axis. Both roll and yaw axes were on the medial plane ($z = 0$). Pitch axis was defined as the line perpendicular to both roll and yaw axes. UB and right forelimb are connected to each other via thoracic muscles, such as *m. rhomboideus* (RH) and *m. serratus ventralis* (SV). UB is subjected to downward gravity force (F_{COM}) and net contractive forces applied by the muscle fascicles, and these forces rotate UB about point P. The rotations of UB about roll, yaw, and pitch axes are shown: (a) default posture with no roll, yaw, and pitch rotations; positive (b) roll, (c) yaw, and (d) pitch. The images were shown in the perspective projections. The three-dimensional musculoskeletal model was constructed using SIMM 6.0.3 (Musculographics Inc.). Abbreviation: *SP*, scapular position.

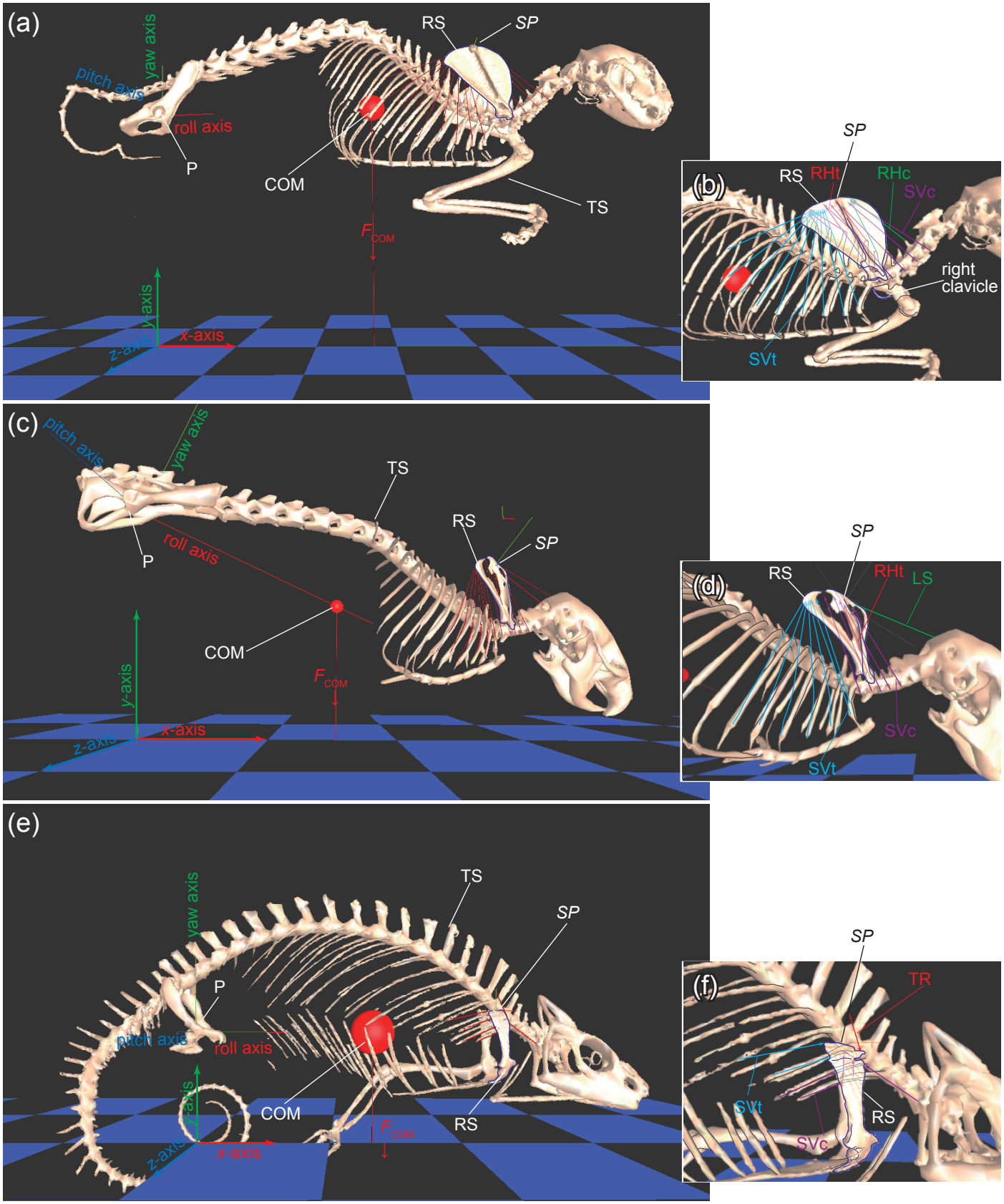

Fig. S11 Rotation models of (a, b) *Felis*, (c, d) *Rattus*, and (e, f) *Chamaeleo*: (a, c, e) musculoskeletal models constructed in SIMM 6.0.3 (Musculographics Inc.); (b, d, f) the arrangements of anti-gravity muscles that originate from the trunk and insert to the top position of the scapula. Uplifted body element (UB) is subjected to the downward gravity force (F_{COM}) at the centre of mass (COM). The musculoskeletal models were constructed in *x*,*y*,*z* coordinate space: *x*, longitudinal; *y*, vertical; and *z*, transverse axes. Abbreviations: COM, centre of mass of the UB; LS, *m. levator scapulae*; P, a common pivot of the UB and TS at the acetabulum; RHc, *m. rhomboideus cervicis*; RHt, *m. rhomboideus thoracis*; RS, right scapula; *SP*, scapular position; SVc, *m. serratus ventralis cervicis*; SVt, *m. serratus ventralis thoracis*; TR, *m. trapezius*; TS, thoracic skeleton. The UB and TS are allowed to rotate freely about the point P, whereas the RS is allowed to translate three-dimensionally along the *x*-, *y*-, *z*-axes. See Table S3 for the muscle fascicle origins and insertions.

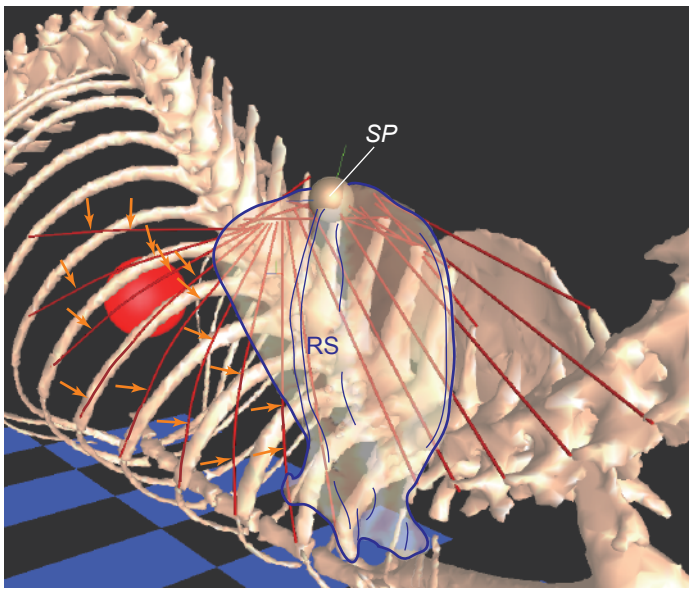

Fig. S12 Paths of the muscle fascicles modeled in the rotation models. The anti-gravity thoracic muscles were modeled to wrap around the rib cage not to run through inside the thoracic skeleton in SIMM 8.0.1. The muscle fascicle paths between the orange colored arrows wrap around the rib cage. Abbreviations: RS, right scapula; *SP*, scapular position.

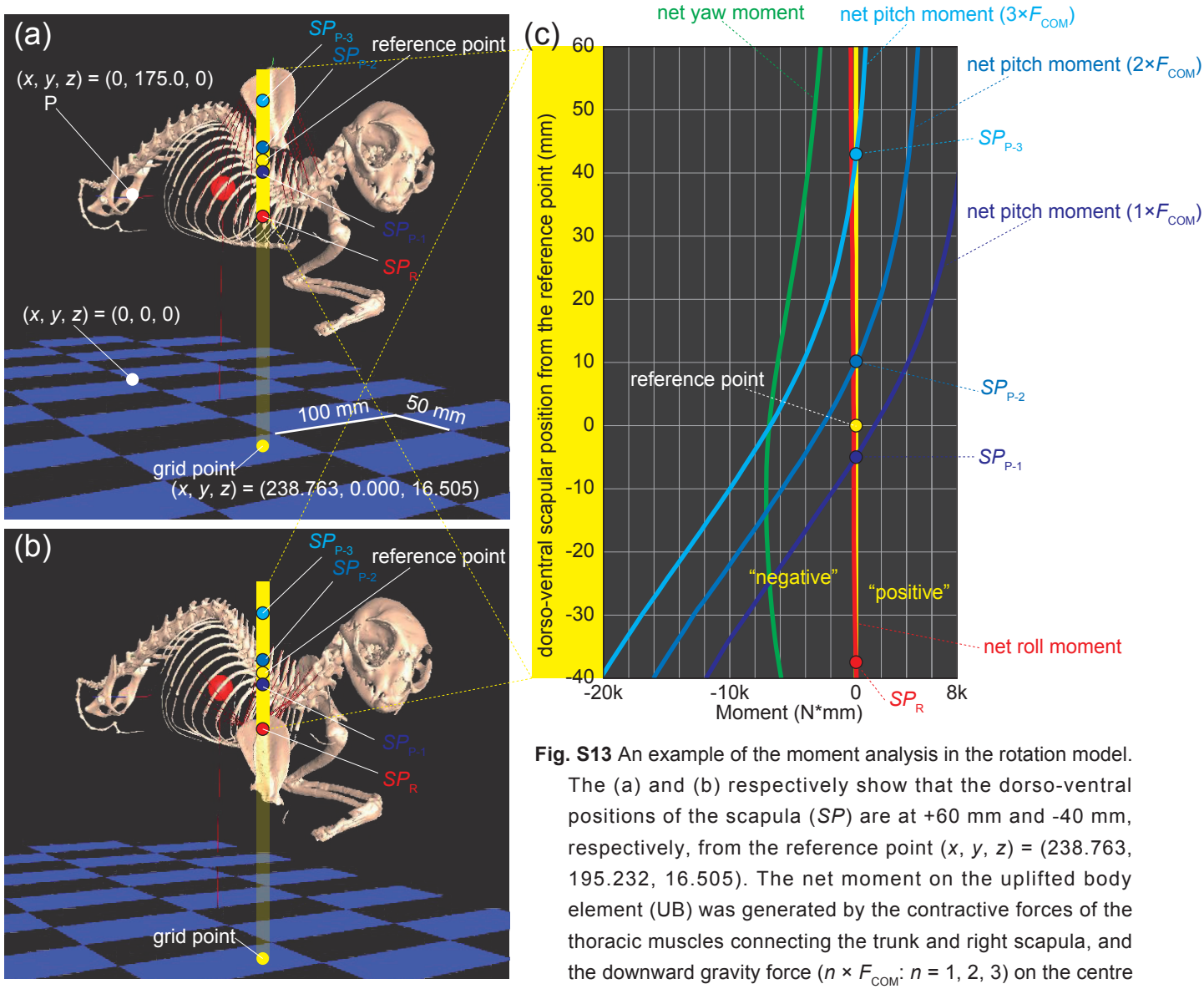

Fig. S13 An example of the moment analysis in the rotation model. The (a) and (b) respectively show that the dorso-ventral positions of the scapula (*SP*) are at +60 mm and -40 mm, respectively, from the reference point (*x*, *y*, *z*) = (238.763, 195.232, 16.505). The net moment on the uplifted body element (UB) was generated by the contractive forces of the thoracic muscles connecting the trunk and right scapula, and the downward gravity force ($n \times F_{COM}$: n = 1, 2, 3) on the centre of mass (COM). (c) Relationships between the net roll, yaw, and pitch moments of the UB and the dorso-ventral scapular position (*SP*) along the line parallel with the *y*-axis through the grid point (*x*, *y*, *z*) = (238.763, 0.000, 16.505) and the reference point. The original point of the *x*, *y*, *z*-coordinate space was defined as the point 175.0 mm beneath the pivot (P) of the UB. *SP* where the net roll, yaw, and pitch moments become zero were respectively defined as SP_R, SP_Y, and SP_P. SP_P estimated for the different $n \times F_{COM}$ (n = 1, 2, 3) was respectively defined as $SP_{P\text{-}1}$, $SP_{P\text{-}2}$, and $SP_{P\text{-}3}$. The range of dorso-ventral position of *SP* shown in (c) corresponds to the yellow bars in (a) and (b).

Table S3 The conditions of the moment analyses. The model used for the analyses, the percentage of the force applied for each muscle fascicles in relation to the possible maximum contractile force (F_{max}), the orientation of the centre of mass acceleration (COM-accel.), and the reference figures for the results of each analysis are shown. See F_{max} in Table S2 for the contractile force of each muscle fascicle. Abbreviations: F_{COM}, downward vertical force on the center of mass; LS, *m. levator scapulae*; RHc, *m. rhomboideus cervicis*; RHt, *m. rhomboideus thoracis*; SVc, *m. serratus ventralis cervicis*; SVt, *m. serratus ventralis thoracis*; TR, *m. trapezius*. The RH and SV were separated into the cervical and thoracic fibres based on its origin.

	analysis	model	LS	RHc	RHt	SVc	SVt	TR	F_{COM}	COM-accel.	result
(a)	vertically-accelerated (control)	*Felis*	—	× 1	× 1	× 1	× 1	—	× 1	vertical	Fig. 4a,d; Fig. S15; Fig. S18a; Fig. S19a
			—	× 1	× 1	× 1	× 1	—	× 2	vertical	Fig. 4a,d
			—	× 1	× 1	× 1	× 1	—	× 3	vertical	Fig. 4a,d ; Fig. S18a
		Rattus	× 1	—	× 1	× 1	× 1	—	× 1	vertical	Fig. 4b,e; Fig. S16
			× 1	—	× 1	× 1	× 1	—	× 2	vertical	Fig. 4b,e
			× 1	—	× 1	× 1	× 1	—	× 3	vertical	Fig. 4b,e
		Chamaeleo	—	—	—	× 1	× 1	× 1	× 1	vertical	Fig. 4c,f; Fig. S17
			—	—	—	× 1	× 1	× 1	× 2	vertical	Fig. 4c,f
			—	—	—	× 1	× 1	× 1	× 3	vertical	Fig. 4c,f
			—	—	—	× 1	× 1	× 1	× 4	vertical	Fig. 4c,f
(b)	anteriorly-accelerated	*Felis*	—	× 1	× 1	× 1	× 1	—	× 1	15° anterior	Fig. S18b
			—	× 1	× 1	× 1	× 1	—	× 3	15° anterior	Fig. S18b
	posteriorly-accelerated	*Felis*	—	× 1	× 1	× 1	× 1	—	× 1	15° posterior	Fig. S18c
			—	× 1	× 1	× 1	× 1	—	× 3	15° posterior	Fig. S18c
	rightward-accelerated	*Felis*	—	× 1	× 1	× 1	× 1	—	× 1	15° rightward	Fig. S18d
			—	× 1	× 1	× 1	× 1	—	× 3	15° rightward	Fig. S18d
	leftward-accelerated	*Felis*	—	× 1	× 1	× 1	× 1	—	× 1	15° leftward	Fig. S18e
			—	× 1	× 1	× 1	× 1	—	× 3	15° leftward	Fig. S18e
(c)	RHc-SVc-dependent	*Felis*	—	× 1	× 0.5	× 1	× 0.5	—	× 1	vertical	Fig. S19b
	RHt-SVt-dependent	*Felis*	—	× 0.5	× 1	× 0.5	× 1	—	× 1	vertical	Fig. S19c
	RHc-RHt-dependent	*Felis*	—	× 1	× 1	× 0.5	× 0.5	—	× 1	vertical	Fig. S19d
	SVc-SVt-dependent	*Felis*	—	× 0.5	× 0.5	× 1	× 1	—	× 1	vertical	Fig. S19e

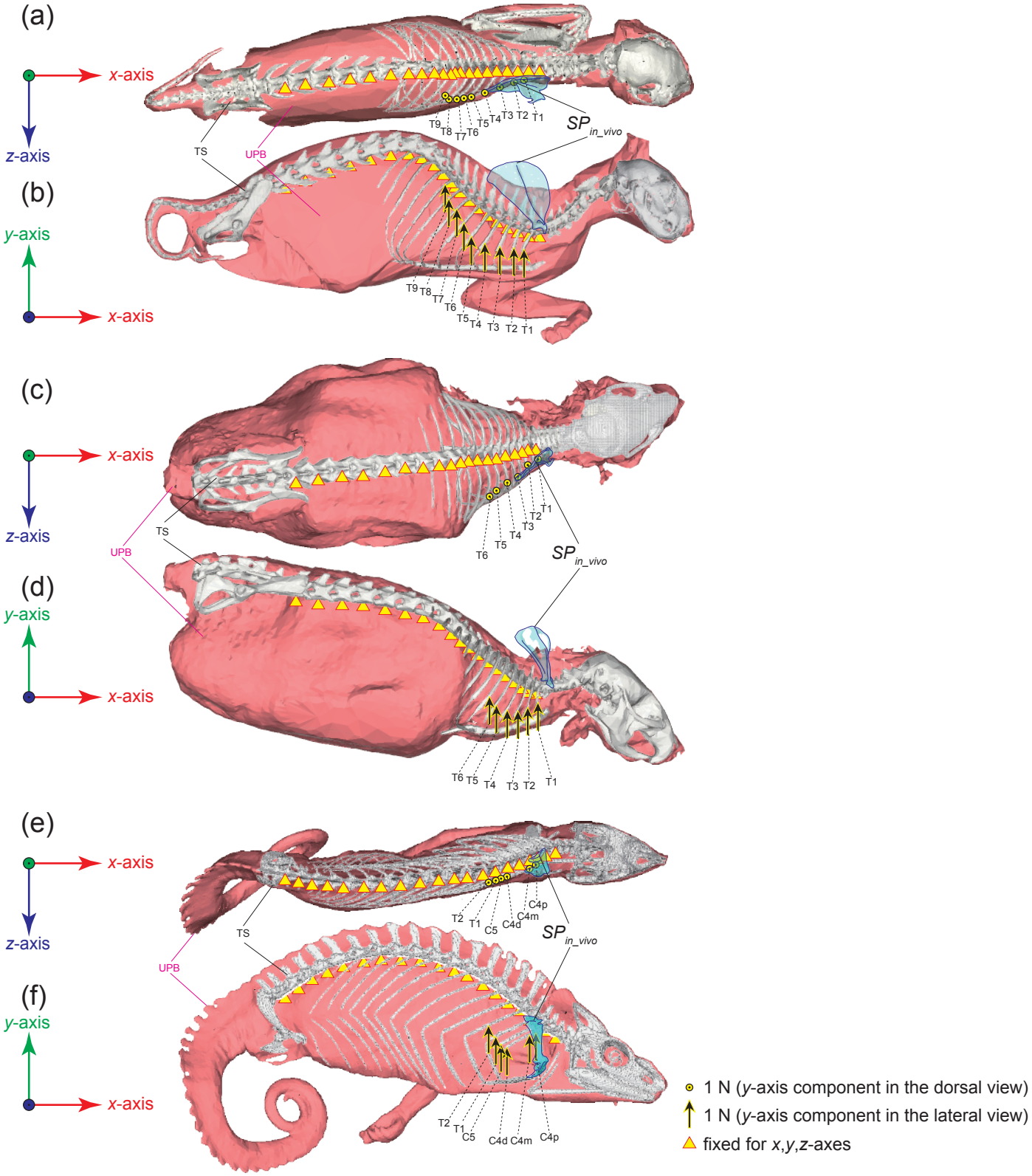

Fig. S14. Boundary conditions of the distortion models in (a, b) *Felis*, (c, d) *Rattus*, and (e, f) *Chamaeleo*: (a, c, e) the dorsal view; (a, c, e) the right lateral view. The thoracic skeleton (TS) of the uplifted body element (UB) was composed of the ~100,000 small cubic voxels. The vertebral column in the trunk was fixed for the *x*,*y*,*z*-axes, and each origins of *m. serratus ventralis* was subjected to a lifting force (1 N) parallel with the *y*-axis. The muscule fascicle origins were indicated as follows: C*n*, origin on the *n*th cervical rib; T*n*, origin on the *n*th thoracic rib. Three fascicle origins occur on the 4th cervical rib of the *Chamaeleo*: proximal (C4p), middle (C4m), and distal (C4d) origins. The scapular positions *in vivo* (SP_{in_vivo}) were based on the literature (*Felis* [Macpherson & Ye, 1998]; *Rattus* [Jenkins, 1974]; *Chamaeleo* [Fischer et al. 2010]: see Fig. S3).

Fig. S15 Thoracic skeleton (TS) of the uplifted body element (UB) and the appropriate scapular positions in support on right forelimb in *Felis*. The scale ball (a sphere in green color; 50 mm in diameter) was set on the origin (*x*, *y*, *z* = 0, 0, 0) of the three-dimensional coordinate space. Three axes through the origin indicate the *x*- (cranio-caudal; red), *y*- (dorso-ventral; green), and *z*- (medio-lateral; blue) axes of the space. The three axes through the common pivot P of the TS and UB indicate the roll (red), yaw (green), and pitch (blue) axes. A sphere in purple indicates centre of mass (COM) of the UB. The distributions of the optimum scapular positions (*SP*), at which the net roll and yaw moments caused by maximum contractive forces of the thoracic muscle fascicles (F_{max}) and gravity force on the COM (F_{COM}) become zero, were respectively indicated in red (SP_R) and green (SP_Y). The *SP*s, at which the net pitch moments generated by the F_{max} the $n \times F_{COM}$ (n = 1, 2, 3) become zero, were respectively indicated in dark blue ($SP_{P\text{-}1}$: n = 1), blue ($SP_{P\text{-}2}$: n = 2), and light blue ($SP_{P\text{-}3}$: n = 3).

Fig. S16 Thoracic skeleton (TS) of the uplifted body element (UB) and the appropriate scapular positions in support on right forelimb in *Rattus*. The scale ball (a sphere in green color; 20 mm in diameter) was set on the origin (*x*, *y*, *z* = 0, 0, 0) of the three-dimensional coordinate space. Three axes through the origin indicate the *x*- (cranio-caudal; red), *y*- (dorso-ventral; green), and *z*- (medio-lateral; blue) axes of the space. The three axes through the common pivot P of the TS and UB indicate the roll (red), yaw (green), and pitch (blue) axes. A sphere in purple indicates centre of mass (COM) of the UB. The distributions of the optimum scapular positions (*SP*), at which the net roll and yaw moments caused by maximum contractive forces of the thoracic muscle fascicles (F_{max}) and gravity force on the COM (F_{COM}) become zero, were respectively indicated in red (SP_R) and green (SP_Y). The *SP*s, at which the net pitch moments generated by the F_{max} the $n \times F_{COM}$ (n = 1, 2, 3) become zero, were respectively indicated in dark blue ($SP_{P\text{-}1}$: n = 1), blue ($SP_{P\text{-}2}$: n = 2), and light blue ($SP_{P\text{-}3}$: n = 3).

Fig. S17 Thoracic skeleton (TS) of the uplifted body element (UB) and the appropriate scapular positions in support on right forelimb in *Chamaeleo*. The scale ball (a sphere in green color; 20 mm in diameter) was set on the origin (*x*, *y*, *z* = 0, 0, 0) of the three-dimensional coordinate space. Three axes through the origin indicate the *x*- (cranio-caudal; red), *y*- (dorso-ventral; green), and *z*- (medio-lateral; blue) axes of the space. The three axes through the common pivot P of the TS and UB indicate the roll (red), yaw (green), and pitch (blue) axes. A sphere in purple indicates centre of mass (COM) of the UB. The distributions of the optimum scapular positions (*SP*), at which the net roll and yaw moments caused by maximum contractive forces of the thoracic muscle fascicles (F_{max}) and gravity force on the COM (F_{COM}) become zero, were respectively indicated in red (SP_R) and green (SP_Y). The *SP*s, at which the net pitch moments generated by the F_{max} the $n \times F_{COM}$ (n = 1, 2, 3) become zero, were respectively indicated in dark blue ($SP_{P\text{-}1}$: n = 1), blue ($SP_{P\text{-}2}$: n = 2), light blue ($SP_{P\text{-}3}$: n = 3), and lighter-most blue ($SP_{P\text{-}4}$: n = 4).

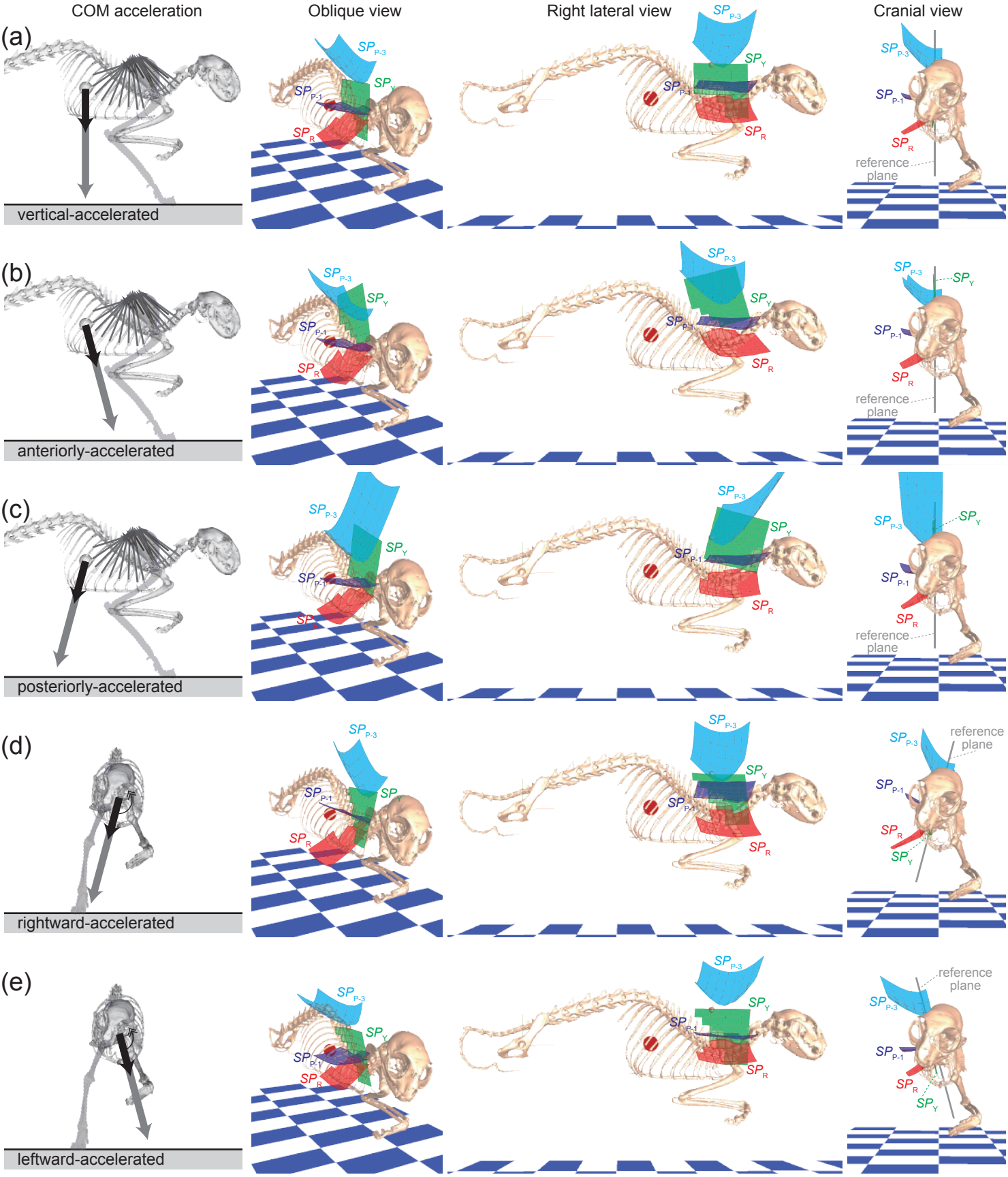

Fig. S18 Appropriate scapular positions (*SP*) estimated for *Felis* in rotation models with the centre of mass (COM) accelerated in different orientations: (a) vertically; and (b) anteriorly-, (c) posteriorly-, (d) rightward-, and (e) leftward-inclined. See Table S3 for the conditions of the analyses. The scapular positions at which the net roll (SP_R), yaw (SP_Y), and pitch ($SP_{P\text{-}n}$) generated by the contractive force of the thoracic muscles and the COM accelerations ($n \times F_{COM}$: n = 1, 3) applied to the fascicle origins and the COM, respectively, become zero were indicated in different colours. The images are shown in orthogonal projection. The reference plane is defined as a plane parallel to the roll and yaw axes of the body element uplifted by the thoracic muscles, which rotates about the acetabulum.

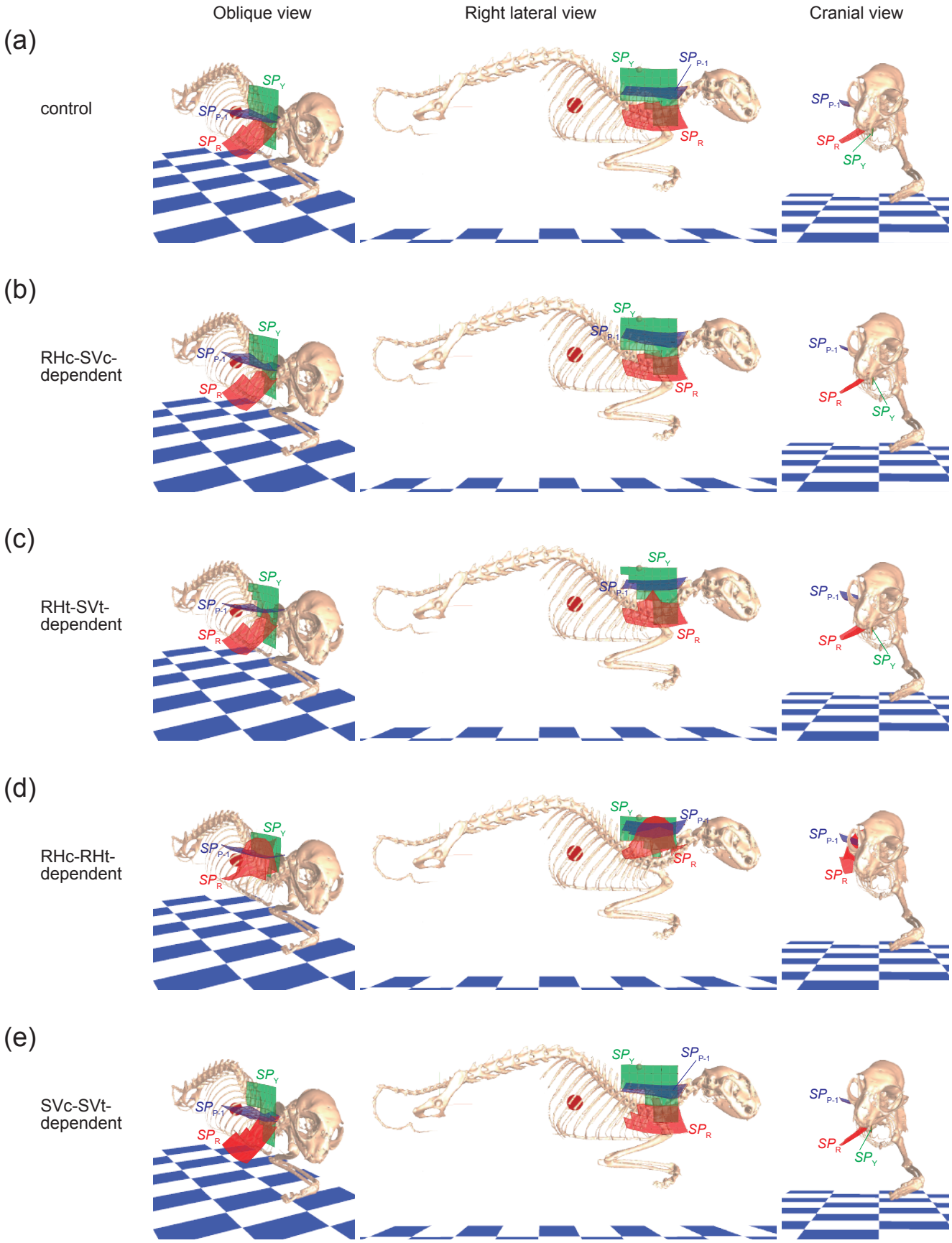

Fig. S19 Appropriate scapular positions (*SP*) estimated for *Felis* in rotation models with the thoracic muscle fascicles activated in different contractile forces. See Table S3a,c for the contractile forces of the thoracic muscles (RHc, *m. rhomboideus cervicis*; RHt, *m. rhomboideus thoracis*; SVc, *m. serratus ventralis cervicis*; SVt, *m. serratus ventralis thoracis*) applied in each model: (a) control (Table S3a); and (b) RHc-SVc-, (c) RHt-SVt-, (d) RHc-RHt-, and (e) SVc-SVt-dependent models. The scapular positions at which the net roll (SP_R), yaw (SP_Y), and pitch ($SP_{P\text{-}n}$) generated by the contractive force of the thoracic muscles and the COM accelerations ($1 \times F_{COM}$) applied to the fascicle origins and the COM, respectively, become zero were indicated in different colours. The images are shown in orthogonal projection.